

Stability of the *Fddd* Phase in Diblock Copolymer Melts

Myung Im Kim,[†] Tsutomu Wakada,[†] Satoshi Akasaka,[†] Shotaro Nishitsuji,[†]
Kenji Saijo,[†] Hirokazu Hasegawa,[†] Kazuki Ito,[‡] and Mikihiro Takenaka^{*,†,‡}

Department of Polymer Chemistry, Graduate School of Engineering, Kyoto University, Kyoto 615-8510,
and Structural Materials Science Laboratory, Spring-8 Center, RIKEN Harima Institute of Research,
1-1-1 Kouto, Sayo-cho, Sayo-gun, Hyogo 679-5148, Japan

Received June 6, 2008; Revised Manuscript Received August 18, 2008

ABSTRACT: The stability of the *Fddd* phase as an equilibrium phase in diblock copolymer melts was examined by using small-angle X-ray scattering and transmission electron microscopy. After 2 days of annealing at 150 °C where *Fddd* was found in a previous study (Takenaka et al. *Macromolecules* 2007, 40, 4399) for the poly(styrene-*block*-isoprene) (S-I), the *Fddd* structure still survived. The thermoreversibility in the order–order transitions (OOTs) between lamella (L) and *Fddd* and between gyroid (G) and *Fddd* was investigated. The long-time annealing at 150 °C induced the transformation from L and G to *Fddd*, indicating that *Fddd* is more stable than L and G at 150 °C. *Fddd* transformed into L and G, respectively, by annealing at 130 and 170 °C. These results supported that the OOTs between L and *Fddd* and between G and *Fddd* are thermoreversible. The stability of the *Fddd* structure after 2 days of annealing and the confirmation of the thermoreversibility in OOTs clarified that the *Fddd* phase exists as an equilibrium phase in S-I diblock copolymer melts.

1. Introduction

A block copolymer exhibits a wide variety of morphologies having long-range order by microphase separation. In diblock copolymer melts, lamella (L), gyroid (G), hexagonally packed cylinder (C), and sphere in the body-centered lattice (S) have been identified as their equilibrium phases.^{1,2} In triblock copolymer melts, many kinds of complex morphologies have been identified extensively. Among them, the *Fddd* phase was first found in poly(isoprene-*block*-styrene-*block*-ethylene oxide) (ISO) triblock copolymer melts by Bailey et al.³ *Fddd* is an orthorhombic structure and single-network structure. Thus, the *Fddd* phase exhibits optical anisotropy and has plateau modulus in linear viscoelasticity due to the network structure. Tyler and Morse calculated the phase diagram of the triblock copolymer melts by using self-consistent field theory (SCFT) and confirmed the *Fddd* phase exists as an equilibrium phase in the triblock copolymer melts.⁴ They also reexamined the phase diagram of diblock copolymer melts, considering the stability of the *Fddd* phase, and found that the *Fddd* phase exists as an equilibrium phase among the L, G, and C phases even in diblock copolymer melts.⁴ In addition, the temperature and composition regions of the *Fddd* phase are also found to be narrow in comparison with the other phases. Yamada et al.⁵ and Ranjan et al.⁶ also found the *Fddd* phase in diblock copolymer melts by using a mode expansion method.

As reported in our previous paper,⁷ we first found the *Fddd* phase in poly(styrene-*block*-isoprene) (S-I) diblock copolymer melts and investigated the morphological change with temperature by using small-angle X-ray scattering (SAXS) and transmission electron microscopy (TEM). We then found the *Fddd* phase exists between the L and G phases and S-I undergoes a L-*Fddd*-G-disorder transition with an increase in temperature. The location of the *Fddd* phase agrees with that calculated by Tyler and Morse qualitatively.

However, recently, Miao and Wickham investigated the thermal fluctuation effect on the phase diagram of diblock copolymer melts and examined the stability of the *Fddd* phase in diblock copolymer melts by using the Landau–Brazovskii

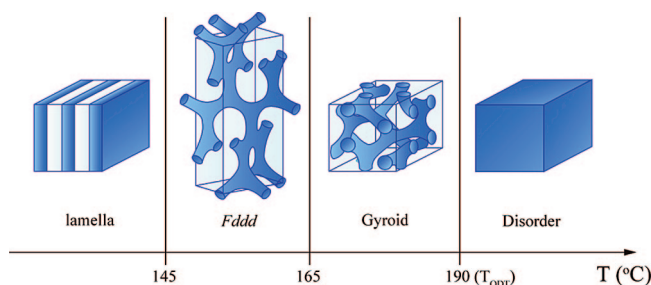


Figure 1. Phase diagram of the S-I diblock copolymer with $M_n = 2.64 \times 10^4$ g/mol and $f_{PI} = 0.629$.

Table 1. Thermal Protocols Used in This Study

thermal protocol I	130 °C, 1 day	→ 150 °C, 2 days	→ 130 °C, 2 days
	↓	↓	↓
	I-a	I-b	I-c
thermal protocol II	170 °C, 1 day	→ 150 °C, 2 days	→ 170 °C, 2 days
	↓	↓	↓
	II-a	II-b	II-c

model.⁸ They claimed that the *Fddd* phase became metastable under strong fluctuation conditions and suggested that the *Fddd* phase we found may be metastable, quoting the metastability of the perforated layer (PL) phase in diblock copolymer melts. The PL phase was first reported as an equilibrium phase in diblock copolymer melts¹ but was found to be a nonequilibrium phase as the result of longer time annealing.⁹ They speculated that the *Fddd* phase in our previous experiment is metastable relative to the G phase, which is similar to the case of the PL phase.

As described in our previous paper, we annealed at each measured temperature for more than 8 h and believe that the diblock copolymer melt reaches its equilibrium phase. However, we cannot eliminate the possibility that the *Fddd* phase is metastable only by the results of the 8 h annealing procedure, and we need to check the stability of the *Fddd* phase extensively in response to their claim. According to their calculation, the region considered as the *Fddd* phase in the previous calculations by Tyler et al. should be a G or L phase and diblock copolymer melts having G or L as the initial morphology do not change their morphologies even after annealing at the temperature region of the *Fddd* phase. Moreover, we cannot expect the

* To whom correspondence should be addressed.

[†] Kyoto University.

[‡] RIKEN Harima Institute of Research.

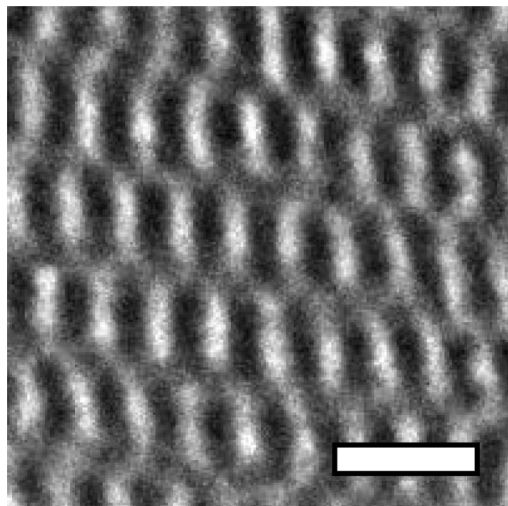


Figure 2. TEM image of the S-I diblock copolymer after 2 days of annealing at 150 °C. Dark parts correspond to the polyisoprene part. The white scale bar corresponds to 50 nm.

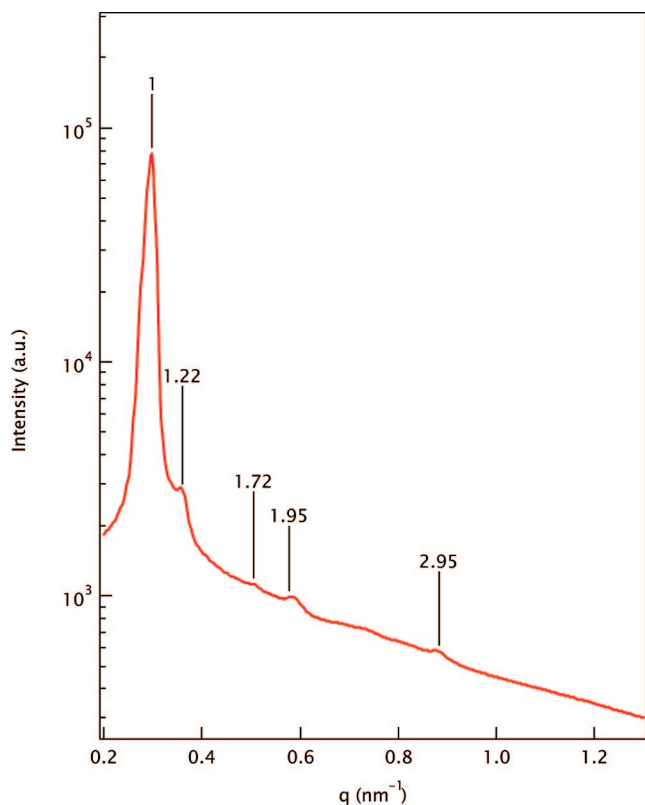


Figure 3. SAXS profile after 2 days of annealing at 150 °C plotted as a function of q .

reversibility of all transitions between L and *Fddd* and between G and *Fddd* if the *Fddd* phase is metastable.

Thus, we examined the following points to check the stability of the *Fddd* phase: (1) long-time annealing at the temperature where *Fddd* appears and check whether *Fddd* still survives after the long-time annealing; (2) thermoreversibility between each phase; we examined the thermoreversibility between L and *Fddd* and between G and *Fddd* in the S-I diblock copolymer.

II. Experimental Method

S-I is the same we used in a previous study. S-I was synthesized by using the anionic polymerization method with *sec*-butyllithium as an initiator and benzene as a solvent. The number-

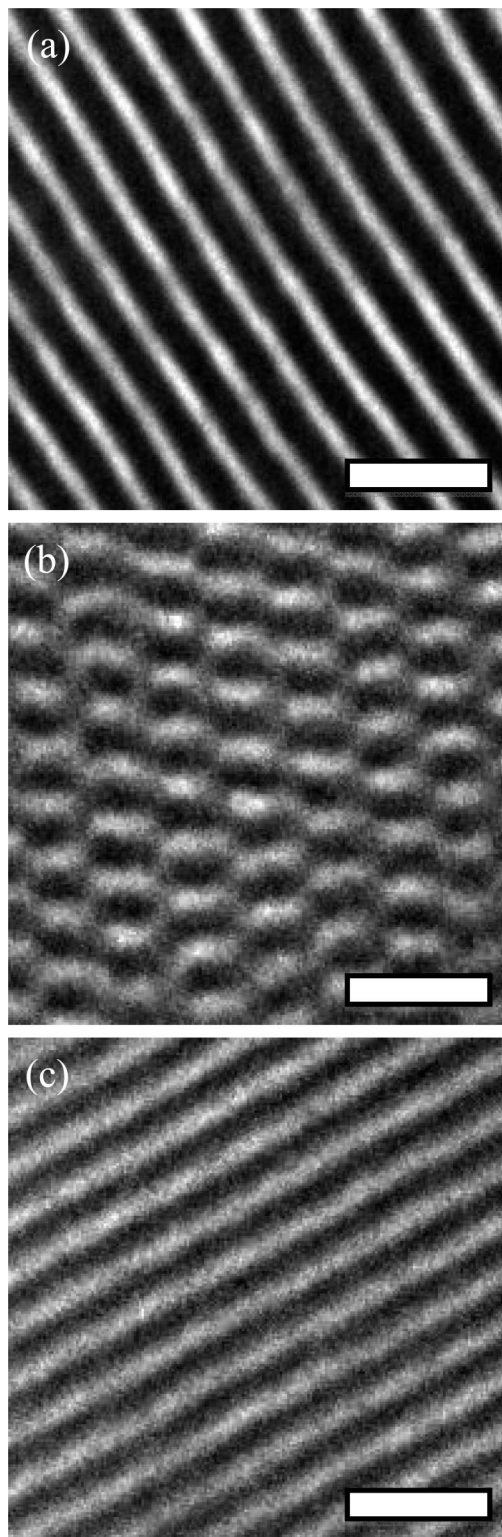


Figure 4. TEM images of the S-I samples after each step during thermal protocol I listed in Table 1: (a) after annealing at 130 °C for 1 day, (b) after annealing at 150 °C for 2 days, and (c) after annealing at 130 °C for 2 days.

averaged molecular weight M_n of S-I is 2.64×10^4 g/mol, and its heterogeneity index $M_w/M_n = 1.02$, where M_w is the weight-averaged molecular weight. The volume fraction of polyisoprene f_{PI} in S-I is 0.629. The temperature ranges of L, *Fddd*, G, and disorder are schematically shown in Figure 1. We dissolved S-I in 5 wt % toluene solvent with 0.2 wt % Irganox and obtained a film by solvent casting at room temperature. The film was dried in a vacuum at room temperature and annealed at 50 °C prior to use.

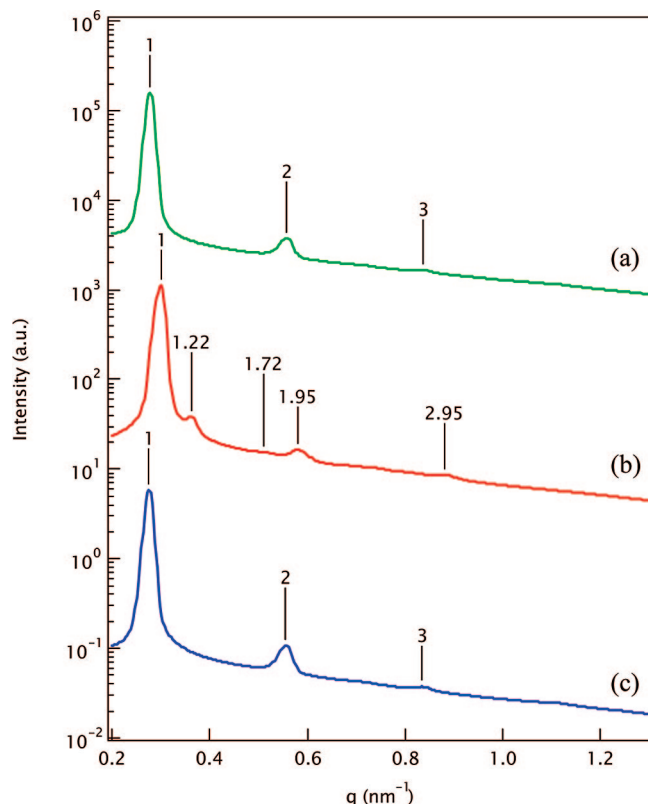


Figure 5. SAXS profiles after each step during thermal protocol I: (a) after annealing at 130 °C for 1 day, (b) after annealing at 150 °C for 2 days, and (c) after annealing at 130 °C for 2 days.

As for the test for long-time annealing, we annealed at 150 °C in a vacuum for 2 days. After annealing, we quenched the S-I sample into iced water and froze the morphology at 150 °C. The frozen morphology was investigated with SAXS and TEM. To check the thermoreversibility between phases, we applied the thermal histories listed in Table 1. After each step, we took a portion of samples, quenched them into iced water, and froze the morphologies at each step for further investigation by SAXS and TEM.

SAXS experiments have been performed at BL45XU in SPring-8.¹⁰ The wavelength is 0.9 Å, and the distance from the sample to the detector is 3.3 m. We used a CCD camera attached with an image intensifier as a detector. The measuring time is 4 s. The obtained data were corrected for air scattering, electrical background, and the distortion due to the CCD camera. Then we circularly averaged the data.

For TEM observation, we microtomed the sample to 50 nm thickness at −80 °C and stained the sample with OsO₄. In the TEM picture, thus, the dark part corresponded to polyisoprene. The TEM observation was performed using a JEM-2000FX with an acceleration voltage of 200 kV.

III. Results and Discussion

III.1. Long-Time Annealing. Figure 2 shows the TEM image of S-I after 2 days of annealing at 150 °C, where *Fddd* was observed in a previous experiment.⁷ In the TEM image, bright ovals are connected by a slightly dark Y-shaped junction to each other. This observed pattern agrees with the images of the *Fddd* structure observed by Bailey et al.³ and Epps et al.^{11–13} The SAXS profile also supports the existence of the *Fddd* structure as shown in Figure 3. The SAXS profile has peaks located at $q/q_m = 1, 1.22, 1.72, 1.95,$ and 2.95 , which agree with those calculated for the *Fddd* structure, where q_m is the q -value at the first-order peak. Thus, the sample kept the *Fddd* structure even after 2 days of annealing.

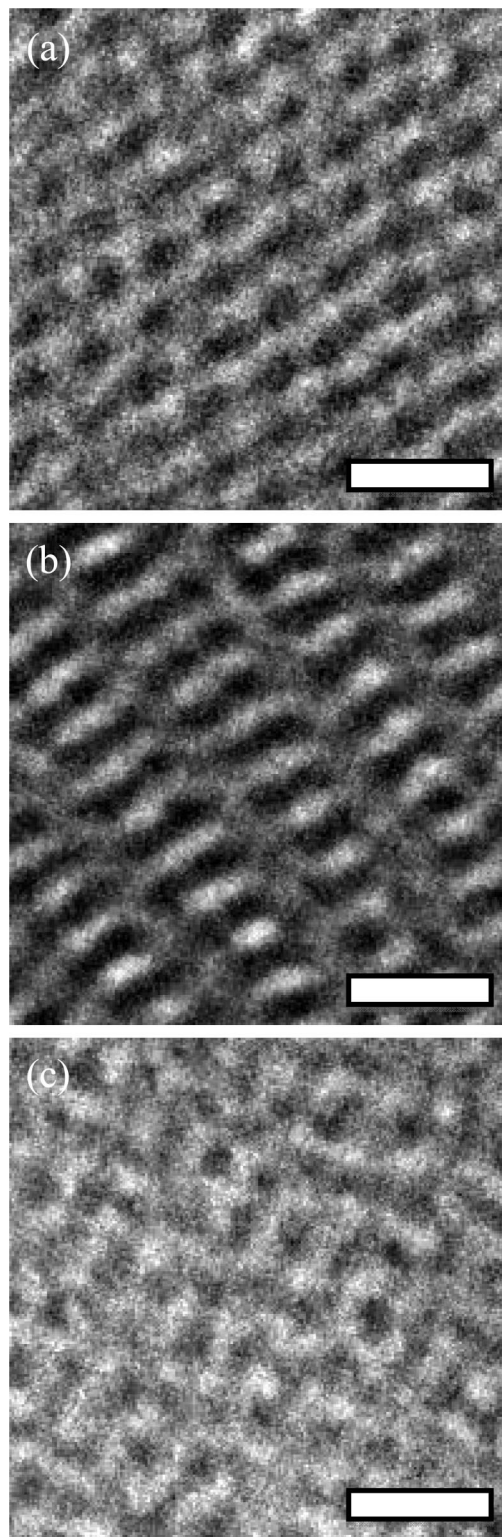


Figure 6. TEM image of the S-I samples after each step during thermal protocol II listed in Table 1: (a) after annealing at 170 °C for 1 day, (b) after annealing at 150 °C for 2 days, and (c) after annealing at 170 °C for 2 days.

III.2. Thermoreversibility between the L and *Fddd* Phases. Figure 4 shows TEM images of the quenched S-I after each step of thermal protocol I listed in Table 1. The lamellar structure is formed during 1 day of annealing at 130 °C (part a). Then after subsequent annealing for 2 days at 150 °C, the TEM image exhibits the representative image of the *Fddd* structure: bright ovals are connected by a trivalent junction. This fact suggests that *Fddd* is more stable than L at 150 °C (Figure

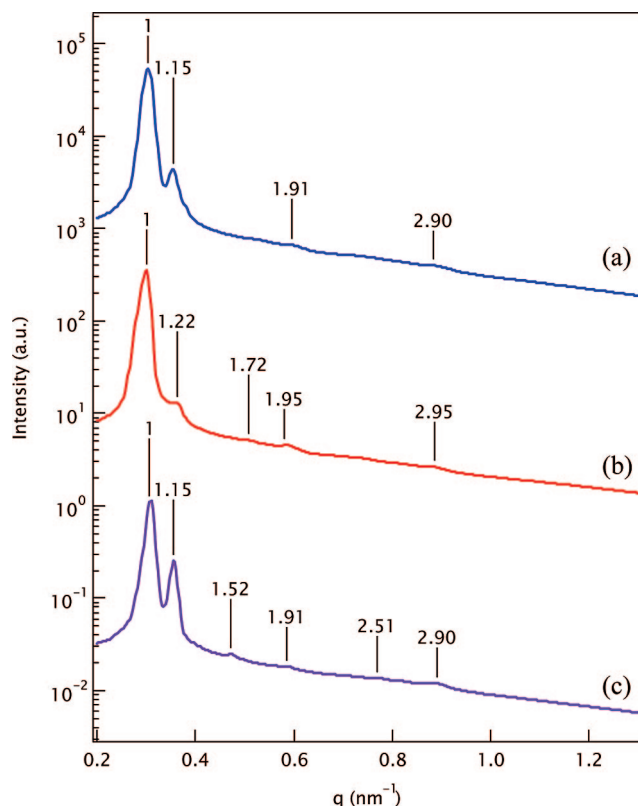


Figure 7. SAXS profiles after each step during thermal protocol II: (a) after annealing at 170 °C for 1 day, (b) after annealing at 150 °C for 2 days, and (c) after annealing at 170 °C for 2 days.

4b). As shown in Figure 4c, annealing at 130 °C for 2 days transformed *Fddd* into L. The SAXS profiles in Figure 5 support the transition between the L and *Fddd* phases. The SAXS profile after annealing at 130 °C has integer high-order peaks ($q/q_m = 1, 2, 3, \dots$), reflecting the lamellar structure (Figure 5a). On the other hand, in the SAXS profile after subsequent annealing at 150 °C, peaks appear at $q/q_m = 1, 1.22, 1.72, 1.95$, and 2.95 , which agree with those of *Fddd* (Figure 5b). The SAXS profile after reannealing at 130 °C is shown in Figure 5c. The peaks appear at $q/q_m = 1, 2, 3, \dots$, which means L is observed. The formation of *Fddd* from L and re-formation of L from *Fddd* indicate that the transition between *Fddd* and L is thermoreversible.

III.3. Thermoreversibility between G and *Fddd*. Figures 6 and 7 display the TEM images and SAXS profiles after each step of thermal protocol II listed in Table 1. After the first step on annealing at 170 °C, the G structure is observed as shown in Figure 6a. The SAXS profile also has peaks at $q/q_m = 1, 1.15, 1.91$, and 2.90 , which agree with those for the G structure (Figure 7a). Thus, annealing at 170 °C induces the formation of the G structure in S-I. After the second step on subsequent annealing at 150 °C, the TEM image in Figure 6b changed into the representative image of the *Fddd* structure. The SAXS profile also changes the peak positions of the *Fddd* structure,

$q/q_m = 1, 1.22, 1.72, 1.95$, and 2.95 (Figure 7b). Thus, the *Fddd* structure is more stable than G at 150 °C. The TEM image and the SAXS profile after the final step, reannealing at 170 °C, are shown in Figures 6c and 7c, respectively. G is observed in the TEM image, and peaks at $q/q_m = 1, 1.15, 1.52, 1.91, 2.51$, and 2.90 are found in the SAXS profile. Thus, by annealing at 170 °C for 2 days the *Fddd* structure changes into G.

The change in the structure on $G \rightarrow Fddd \rightarrow G$ according to thermal protocol II proves that the order–order transition between G and *Fddd* is thermoreversible. As described in section III.2, *Fddd* is more stable than L at 150 °C, and here we show *Fddd* is more stable than G at 150 °C. Thus, we can conclude that the *Fddd* phase exists as an equilibrium phase between L and G of the S-I diblock copolymer melts.

Thermoreversibility between L and *Fddd* and between G and *Fddd* is confirmed in the above experiment. This confirmation supports that *Fddd* is an equilibrium phase.

IV. Conclusion

We examined whether the *Fddd* phase identified in our previous study exists as an equilibrium phase. We applied 2 days of annealing at 150 °C, where *Fddd* was found in the S-I diblock copolymer, and observed the morphology by SAXS and TEM. The *Fddd* structure remained after annealing. We also check that the OOTs between L and *Fddd* and between G and *Fddd* are thermoreversible. L and G can be transformed into the *Fddd* structure by annealing at 150 °C, indicating that *Fddd* is more stable than L and G at 150 °C. *Fddd* can change into L and G, respectively, by annealing at 130 and 170 °C, supporting that the OOTs between L and *Fddd* and between G and *Fddd* are thermoreversible. The unchanged *Fddd* structure after 2 days of annealing and the confirmation of the thermoreversibility in OOTs clarify that the *Fddd* phase exists as an equilibrium phase in S-I diblock copolymer melts.

References and Notes

- (1) Khandpur, A. K.; Forster, S.; Bates, F. S.; Hamley, I. W.; Ryan, A. J.; Bras, W.; Almdal, K.; Mortensen, K. *Macromolecules* **1995**, *28* (26), 8796.
- (2) Matsen, M. W.; Schick, M. *Phys. Rev. Lett.* **1994**, *72* (16), 2660.
- (3) Bailey, T. S.; Hardy, C. M.; Epps, T. H.; Bates, F. S. *Macromolecules* **2002**, *35* (18), 7007.
- (4) Tyler, C. A.; Morse, D. C. *Phys. Rev. Lett.* **2005**, *94* (20), 208302.
- (5) Yamada, K.; Nonomura, M.; Ohta, T. *J. Phys.: Condens. Matter* **2006**, *18* (32), L421.
- (6) Ranjan, A.; Morse, D. C. *Phys. Rev. E* **2006**, *74* (1), 011803.
- (7) Takenaka, M.; Wakada, T.; Akasaka, S.; Nishitsuji, S.; Saijo, K.; Shimizu, H.; Kim, M. I.; Hasegawa, H. *Macromolecules* **2007**, *40* (13), 4399.
- (8) Miao, B.; Wickham, R. A. *J. Chem. Phys.* **2008**, *128* (5), 054902.
- (9) Hajduk, D. A.; Takenouchi, H.; Hillmyer, M. A.; Bates, F. S.; Vigild, M. E.; Almdal, K. *Macromolecules* **1997**, *30* (13), 3788.
- (10) Fujisawa, T.; Inoue, K.; Oka, T.; Iwamoto, H.; Uruga, T.; Kumasaka, T.; Inoko, Y.; Yagi, N.; Yamamoto, M.; Ueki, T. *J. Appl. Crystallogr.* **2000**, *33* (1), 797.
- (11) Epps, T. H.; Bates, F. S. *Macromolecules* **2006**, *39* (7), 2676.
- (12) Epps, T. H.; Cochran, E. W.; Bailey, T. S.; Waletzko, R. S.; Hardy, C. M.; Bates, F. S. *Macromolecules* **2004**, *37* (22), 8325.
- (13) Epps, T. H.; Cochran, E. W.; Hardy, C. M.; Bailey, T. S.; Waletzko, R. S.; Bates, F. S. *Macromolecules* **2004**, *37* (19), 7085.

MA801268D